

Molecular mechanism of complement inhibition by the trypanosome receptor ISG65

Alexander D Cook^{1,2}, Mark Carrington^{3*}, Matthew K Higgins^{1,2*}

¹Department of Biochemistry, University of Oxford, Oxford, United Kingdom; ²Kavli Institute for Nanoscience Discovery, Dorothy Crowfoot Hodgkin Building, University of Oxford, Oxford, United Kingdom; ³Department of Biochemistry, University of Cambridge, Cambridge, United Kingdom

Abstract African trypanosomes replicate within infected mammals where they are exposed to the complement system. This system centres around complement C3, which is present in a soluble form in serum but becomes covalently deposited onto the surfaces of pathogens after proteolytic cleavage to C3b. Membrane-associated C3b triggers different complement-mediated effectors which promote pathogen clearance. To counter complement-mediated clearance, African trypanosomes have a cell surface receptor, ISG65, which binds to C3b and which decreases the rate of trypanosome clearance in an infection model. However, the mechanism by which ISG65 reduces C3b function has not been determined. We reveal through cryogenic electron microscopy that ISG65 has two distinct binding sites for C3b, only one of which is available in C3 and C3d. We show that ISG65 does not block the formation of C3b or the function of the C3 convertase which catalyses the surface deposition of C3b. However, we show that ISG65 forms a specific conjugate with C3b, perhaps acting as a decoy. ISG65 also occludes the binding sites for complement receptors 2 and 3, which may disrupt recruitment of immune cells, including B cells, phagocytes, and granulocytes. This suggests that ISG65 protects trypanosomes by combining multiple approaches to dampen the complement cascade.

eLife assessment

This **fundamental** study significantly advances our understanding of how parasites evade the host complement immune system. The new cryo-EM structure of the trypanosome receptor ISG65 bound to complement component C3b is highly **compelling** and well-supported by biochemical experiments. This work will be of broad interest to parasitologists, immunologists, and structural biologists.

Introduction

African trypanosomes can survive in the blood and tissue spaces of mammals for decades (*Sudarshi et al., 2014*), despite constant exposure to the molecules and cells of the immune system. They have evolved a unique surface coat packed with many copies of a single variant surface glycoprotein (VSG) (*Schwede et al., 2015*). At a population level, antigenically distinct VSGs are expressed over the course of an infection, thereby preventing antibody-mediated clearance (*Schwede and Carrington, 2010*). In addition to the need to resist acquired immunity, trypanosomes must also evade innate immune processes, such as the complement system. Recent studies have identified receptors which function within the trypanosome surface coat and which bind to either complement factor C3b (*Macleod*

*For correspondence:

mc115@cam.ac.uk (MC);
matthew.higgins@bioch.ox.ac.uk (MKH)

Competing interest: The authors declare that no competing interests exist.

Funding: See page 12

Preprint posted

27 April 2023

Sent for Review

01 May 2023

Reviewed preprint posted

12 July 2023

Reviewed preprint revised

05 April 2024

Version of Record published

24 April 2024

Reviewing Editor: Jungsan Sohn, Johns Hopkins University School of Medicine, United States

© Copyright Cook et al. This article is distributed under the terms of the [Creative Commons Attribution License](https://creativecommons.org/licenses/by/4.0/), which permits unrestricted use and redistribution provided that the original author and source are credited.

et al., 2022) or complement modulator factor H (*Macleod et al., 2020*). ISG65 was identified as the trypanosome C3b receptor and has been shown to reduce the susceptibility of trypanosomes to antibody-mediated clearance in a mouse infection model (*Macleod et al., 2022*). However, we have little insight into the molecular mechanisms underpinning complement resistance mediated by ISG65.

The complement system involves a complex set of molecular cascades (*Gros et al., 2008; Zipfel et al., 2013*). These come together at the conversion of serum complement C3 into C3b and the deposition of C3b on a pathogen surface through the formation of a thioester bond between the TED domain of C3b and cell surface components (*Ricklin et al., 2016*). C3b deposition can occur through three major and distinct pathways. In the classical pathway, antibodies mediate the recruitment of C3b, while in the lectin pathway, this results from the recognition of cell surface glycans. In both cases, these events establish C4bC2b convertases, which catalyse the conversion of C3 into C3b and its surface deposition. In contrast, the alternative pathway involves stochastic conversion of C3 into C3b, resulting in an initial deposition event independent of other molecular recognition processes (*Nilsson and Nilsson Ekdahl, 2012*). The first deposited C3b molecules can then assemble with factors B and D, leading to formation of the C3 convertase, C3bBb, which catalyses deposition of further C3b molecules and amplification of downstream responses (*Roijakkers et al., 2009*).

The outcomes of C3b deposition are also diverse, involving both the cellular and molecular branches of the immune system. Direct recognition of immobilised C3b, or its cleavage products iC3b, C3dg, and C3d, by complement receptors stimulates the activity of various immune cells. Complement receptor 1 (CR1) is found on macrophages and binding of CR1 to C3b promotes phagocytosis of pathogens such as *Leishmania* (*Rosenthal et al., 1996*). Complement receptor 2 (CR2) is found on B cells and forms a signal-transducing B cell co-receptor with CD19 and CD81 (*Bradbury et al., 1992*). CR2-CD19-CD81 is stimulated upon binding to C3d, and the absence of CR2 severely attenuates humoral immunity (*Fischer et al., 1998; Croix et al., 1996*). Complement receptors 3 and 4 are integrins found on various leukocytes and are associated with diverse effects, such as enhancement of natural killer cell cytotoxicity and antibody-dependent eosinophil cytotoxicity against schistosomes (*Erdei et al., 2019; Capron et al., 1987*). Through mechanisms distinct from those mediated by complement receptors, C3b can trigger a cascade which leads to recruitment of the pore-forming membrane attack complex (*Tegla et al., 2011*). Here, deposited C3b binds to other complement factors, resulting in formation of a C5 convertase. This cleaves complement factor C5, generating C5b, which recruits factors C6 and C7 to cause membrane association. Factors C8 and C9 can then bind to C5b7 on the pathogen surface, leading to the formation of a pore which mediates cell death (*Couves et al., 2023*).

Pathogens have evolved a wide range of different approaches to evade complement-mediated destruction by regulating different stages of the complement cascade (*Zipfel et al., 2013; Lambris et al., 2008*). These include *S. aureus* Efb-C which binds to the TED domain of C3 and prevents the conformational change required to generate C3b (*Hammel et al., 2007*); *S. aureus* Efb, Ehp, and Sbi which bind to the TED domain of C3/C3d and prevent binding of complement receptor 2, thereby inhibiting B cell recruitment (*Ricklin et al., 2008; Iseman et al., 2010*); smallpox virus SPICE which displaces factor B, preventing C3 convertase function (*Forneris et al., 2010*); and *S. aureus* SCIN and Sbi which bind to the C3bBb C3 convertase and hold it in an inactive conformation (*Roijakkers et al., 2009; Clark et al., 2011*). This, therefore, raised the question of how ISG65 regulates complement-mediated processes. Does it inhibit the deposition of C3b by preventing the function of C3 convertases? Does it block the recognition of C3b by complement receptors, thereby reducing recruitment of immune cells? Does it block the function of the C5 convertase, preventing formation of the membrane attack complex? Here, we combine structural biology and biophysical methods to show that ISG65 does not block C3 convertase formation, but instead may combine multiple functionalities to dampen the outcomes of C3b deposition.

Results

Two distinct binding sites connect C3b to ISG65

We previously determined the crystal structure of ISG65 bound to C3d (equivalent to the TED domain of C3b), revealing how the three core helices of ISG65 form a concave surface to which C3d binds (*Macleod et al., 2022*). However, this study also showed that this structure does not reveal the full

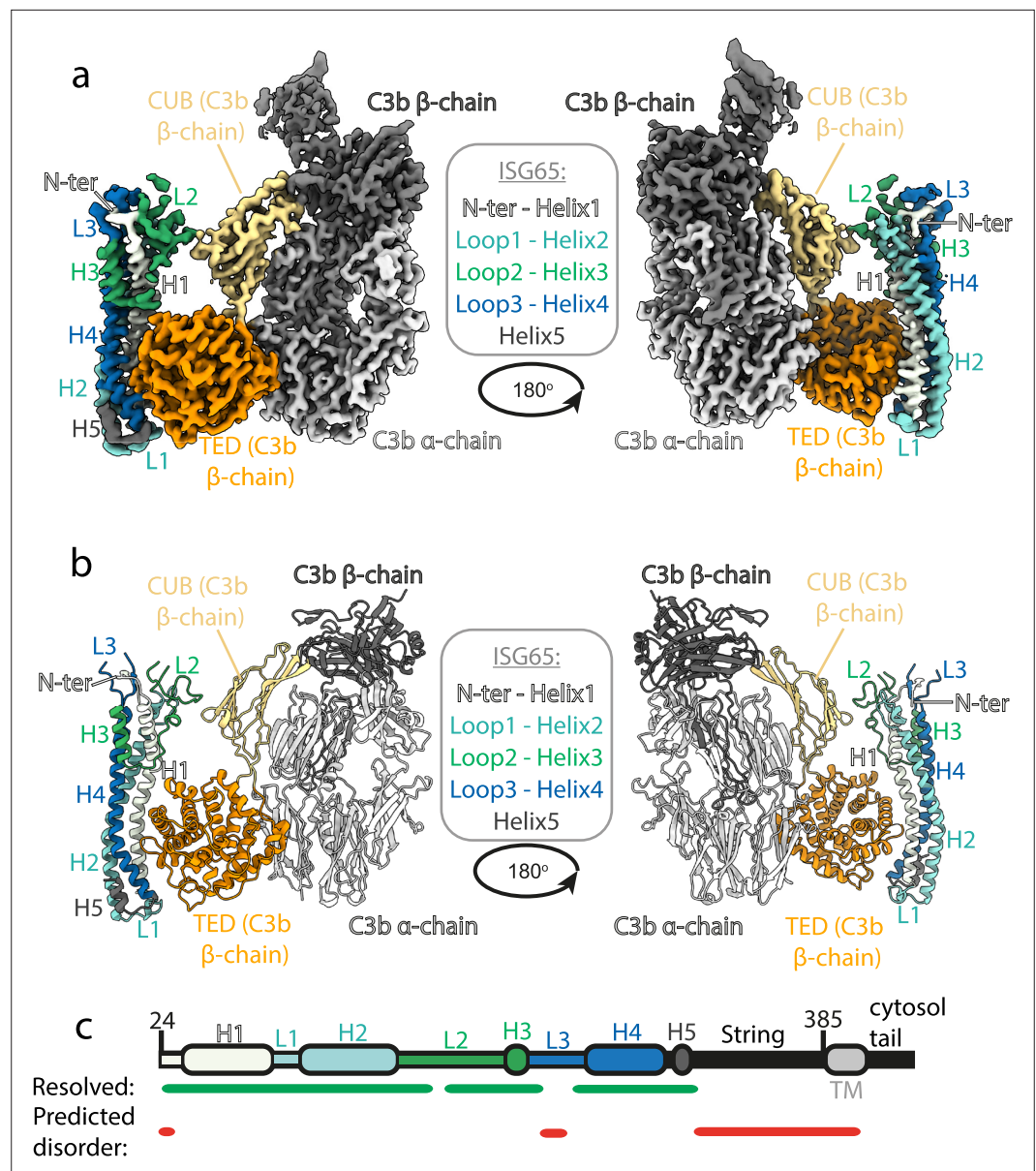


Figure 1. Structure of the complex between ISG65 and human C3b. **(a)** Composite volume of locally refined regions determined using cryogenic electron microscopy for ISG65 bound to human C3b. ISG65 is coloured in different shades of blue and green, as indicated in the legend in the centre of the panel (loop1 and helix 2 are light blue, loop 2 and helix 3 are green and loop 3 and helix 4 are dark blue). C3b is coloured in grey scale with the α -chain in light grey and the β -chain in dark grey. The TED domain is highlighted in orange and the CUB domain highlighted in yellow. **(b)** Molecular model of the same complex with a colour scheme matching that of **(a)**. **(c)** A schematic showing the features of ISG65, coloured as **(a)**. Regions resolved in the structure are indicated underneath the schematic using a green line and regions predicted to be disordered using AUCpreD (Wang *et al.*, 2016) are shown by the red line.

The online version of this article includes the following figure supplement(s) for figure 1:

Figure supplement 1. Workflow of Cryo-EM data processing.

interaction interface between ISG65 and C3b. Surface plasmon resonance had been used to measure the affinities of ISG65 for the different fragments of C3, C3b, and C3d (Macleod *et al.*, 2022). C3b exhibited a higher affinity for C3b than C3d, suggesting that ISG65 forms contacts with C3b in addition to those structurally characterised with the TED domain.

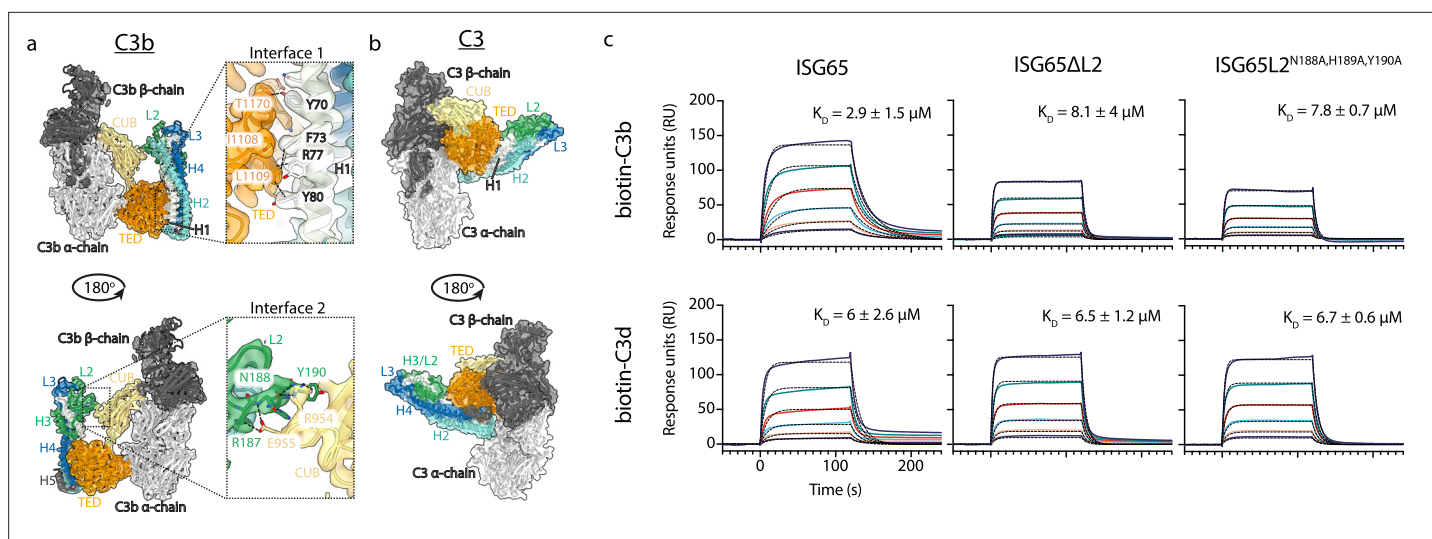


Figure 2. ISG65 forms two distinct interfaces with the TED and CUB domains of C3b. **(a)** The ISG65-C3b model shown in transparent cryo-EM density. The top panel shows the interface between ISG65 and the TED domain (orange), with bottom panel showing the interface between loop L2 of ISG65 (green) and the CUB domain of C3b (yellow). In each case, the left-hand panel shows the intact structure, with a dotted box highlighting the region shown in an enlarged form in the right-hand panel. **(b)** The ISG65 model superimposed onto a previously determined structure of C3 (PDB ID: 2A73) (*Janssen et al., 2005*) via the TED domain of the ISG65-C3b model. This is shown as a ribbon within a transparent surface representation. ISG65 can bind to C3 via the TED domain, via the same interface as previously identified for ISG65-C3d (*Macleod et al., 2022*). **(c)** Surface plasmon resonance data showing responses from the injection of ISG65, ISG65 Δ L2, and ISG65^{N188A,H189A,Y190A} (twofold serial dilutions from a concentration of 10 μ M) over a flow cell coupled to biotin-C3b or biotin-C3d. Data is representative of three experimental repeats. Raw data is available in **Figure 2—source data 1**.

The online version of this article includes the following source data and figure supplement(s) for figure 2:

Source data 1. Surface plasmon resonance data.

Figure supplement 1. Surface plasmon resonance data.

Figure supplement 1—source data 1. Surface plasmon resonance data.

Figure supplement 1—source data 2. Surface plasmon resonance data.

To provide a full molecular model of ISG65 bound to C3b we used cryogenic electron microscopy (**Figure 1**). We prepared ISG65-C3b complex in the presence of fluorinated octyl maltoside, which improved particle distribution in grids while avoiding dissociation of the complex. We collected 14,339 movies from which particles were extracted and a three-dimensional volume was calculated. To improve the resolution of the region containing the binding site, local refinement was performed using a mask covering ISG65 and the TED and CUB domains of C3b, resulting in a volume at 3.4 Å resolution. Guided by previous structures of ISG65 (*Macleod et al., 2022*) and C3b (*Janssen et al., 2006*) and by an AlphaFold2 (*Jumper et al., 2021*) model of ISG65, we were able to build a molecular model for the ISG65-C3b complex (**Figure 1**, **Figure 1—figure supplement 1**, **Supplementary file 1**).

This structure reveals the two distinct interfaces formed between ISG65 and C3b (**Figure 1**, **Figure 2a**). The first of these, interface 1, matches that previously identified through our crystallographic analysis (*Macleod et al., 2022*), with no significant differences between the models in this region. While our previous structure did not have interpretable electron density for loops L2 and L3, perhaps due to their disorder, or due to proteolysis during crystallisation, most of L2 and parts of L3 were ordered and resolved in our cryogenic electron microscopy-derived volume. This allowed us to build a de novo model for residues 179–212 of L2. In particular, L2 directly contacts the CUB domain of C3b, with an electrostatic interaction centered around C3b residue Arg954. Docking suggests that this second interface does not form between ISG65 and C3, as also seen in a recent structure of ISG65 bound to C3b (*Sülzen et al., 2023*; **Figure 2b**). The presence of this additional contact between ISG65 and C3b, which is not present between ISG65 and the TED domain alone, explains the differences in affinity of ISG65 for C3, C3b, and C3d.

We, and others, had previously used surface plasmon resonance analysis to measure the binding of C3, C3b, and C3d to immobilised biotinylated ISG65 (*Macleod et al., 2022*; *Sülzen et al., 2023*;

Lorentzen et al., 2023). However, we were concerned that differences in size and shape between the C3 variants might cause them to interact differently in this assay due to differences in hydrodynamic properties affecting their on-rates. To reliably compare ISG65 variants, we, therefore, changed to an assay in which C3b and C3d were conjugated to the chip surface, allowing us to flow the same ISG65 samples over these surfaces. To conjugate C3b and C3d in a manner which closely matches their orientation when conjugated to a pathogen, we chemically biotinylated Cys1010 and captured it on a streptavidin-coated chip. ISG65 was flowed over immobilised biotinylated C3b and biotinylated C3d, showing binding which fitted a one-to-one binding model with an affinity of 2.9 μM for C3b, and 6 μM for C3d (**Figure 2, Figure 2—figure supplement 1**). As C3d contains all determinants for formation of interface 1, we attribute the greater affinity for C3b over C3d to the contacts formed in interface 2. Indeed, we next generated two mutant forms of ISG65 in which we aimed to disrupt interface 2, either through deletion of loop 2 (ISG65 ΔL2), or through mutation of the three ISG65 residues in loop 2 which mediate interface 2 (ISG65L2^{N188A,H189A,Y190A}). In neither case did these mutations affect the affinity for C3d but both mutations reduced the affinity for C3b to match that for C3d, supporting the model in which interface 2 forms with C3b but not C3d (**Figure 2, Figure 2—figure supplement 1**).

ISG65 does not inhibit formation of the C3 convertase but does form a specific covalent conjugate with C3b

In addition to determining the structure of C3b bound to ISG65, the same data set also yielded a three-dimensional class consisting of a structure of C3b which lacked density for ISG65 and was indistinguishable from previous C3b structures. This allowed us to determine whether the presence of ISG65 caused a conformational change in C3b (**Figure 3a**). Fitting the model of the C3b-ISG65 complex (without ISG65) into the volume derived for the complex resulted in a map-model correlation of 0.79. When we fitted the same model into the volume derived from C3b alone, the correlation was 0.76, indicating that the ISG65-bound conformation of C3b is equivalent to the free conformation of C3b. Therefore, unlike bacterial C3b-effector proteins, such as Efb-C (*Hammel et al., 2007*), ISG65 does not prevent C3 from adopting the active conformation of C3b. Indeed, this is consistent with ISG65 binding to C3b that is already conjugated to the trypanosome surface, rather than preventing C3b formation.

The initial conjugation of C3b to the trypanosome surface is followed by formation of the C3 convertase, consisting of C3b bound to factor Bb (C3bBb). This requires factor B to first bind to C3b and then be cleaved by factor D to generate C3bBb. In order to determine whether ISG65 can block C3bBb formation, we first compared the ISG65-C3b structure with those of C3b bound to factors B and D³⁰. This indicates that ISG65 does not compete with either factor B or Factor D and does not block the binding of factor B (**Figure 3b**). This suggests that the C3 convertase can form in the presence of ISG65.

We, therefore, developed an in vitro assay for C3 convertase formation in which we combined C3 and factor B with catalytic quantities of C3b and factor D. When mixed in vitro, this triggered the cleavage of C3 to C3b, as shown by the production of C3a. In addition, it resulted in the cleavage of factor B to form Bb and Ba (**Figure 3c**). When performed with addition of a greater than three-fold excess of ISG65, the production of C3a and Ba were unaltered, indicating that formation of the C3bBb C3 convertase can proceed in the presence of ISG65. (**Figure 3c**). Indeed, two other recent reports also indicate that ISG65 does not affect formation of the C3 convertase (*Sülzen et al., 2023; Lorentzen et al., 2023*).

Comparison of the outcome of C3 convertase formation in the presence and absence of ISG65, revealed that the presence of ISG65 resulted in a high molecular weight band, which we identified through mass spectrometry to be a conjugate of ISG65 with C3b (**Figure 3c, Supplementary file 3**). When we conducted the equivalent experiment using the same amount of bovine serum albumin instead of ISG65, we did not observe the formation of this conjugate, suggesting that it occurs specifically due to the proximity of ISG65 and the thioester-forming residue of C3b when in the complex (**Figure 3d**). Finally, to identify which region of ISG65 is responsible for the formation of this conjugate, we used versions of ISG65 which lack loops L1, L2, or L3, or which lacked the flexible C-terminal region (ΔC). In each of the loop mutants, we still observed the formation of the ISG65-C3b conjugate. However, this was not observed in the ΔC mutant (**Figure 3e**). This C-terminal region is an unstructured string of 72 amino acids that does not form part of the binding site for C3b and is not

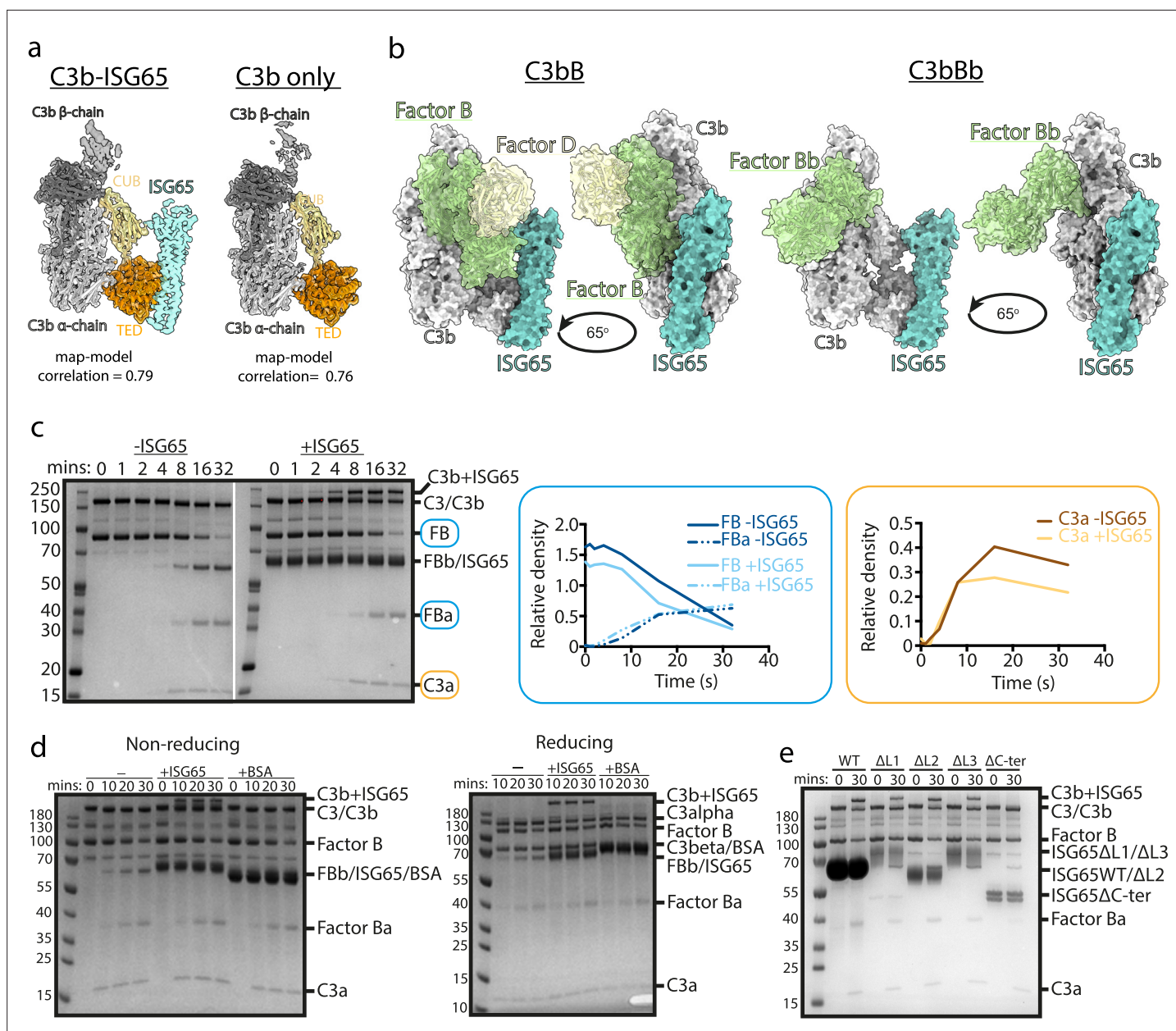


Figure 3. ISG65 does not block the formation of the C3 convertase. **(a)** The structure of the ISG65-C3b complex (without ISG65) docked into the electron microscopy-derived volumes obtained for the ISG65-C3b complex (left) and C3b alone (right). **(b)** Composite models obtained by docking the C3b-ISG65 structure onto those of C3b bound to factors B and D (PDB ID: 2XWJ) (Forneris *et al.*, 2010) or factor Bb (6RUR) (Rooijakkers *et al.*, 2009). **(c)** An assay for C3 convertase formation in which C3b and factor D were each added at concentrations of 12 nM and C3 and factor B at concentrations of 600 nM. Samples were taken at different time points and were analysed by SDS-PAGE analysis with Coomassie staining. This was done in the absence (left-hand gel) and presence (right-hand gel) of 2 μ M ISG65. The graphs show quantification by densitometry for factors B, Ba and C3a to assess convertase function. **(d)** An equivalent assay to that shown in **(c)**, conducted in the absence of non-complement protein (left), or the presence of 2 μ M ISG65 (central) or 2 μ M BSA (right). The left-hand gel was run in non-reducing conditions while the right-hand gel was run in reducing conditions. **(e)** An equivalent assay to that shown in **(c)**, conducted in presence of 2 μ M ISG65 or of ISG65 variants lacking loop 1 (Δ L1), loop 2 (Δ L2), loop 3 (Δ L3) or the extended disordered C-terminal region (Δ C-ter). Raw data available [Figure 3—source data 1](#).

The online version of this article includes the following source data for figure 3:

Source data 1. [Figure 3c](#) – raw gel 1 annotated.

Source data 2. [Figure 3c](#) – raw gel 1.

Source data 3. [Figure 3c](#) – raw gel 2 annotated.

Source data 4. [Figure 3c](#) – raw gel 2.

Figure 3 continued on next page

Figure 3 continued

Source data 5. Figure 3d – raw gel annotated.

Source data 6. Figure 3d – raw gel.

Source data 7. Figure 3e – raw gel annotated.

Source data 8. Figure 3e – raw gel.

observed in the structures. It is predicted to form a flexible linker which connects the structured ISG65 domain to the plasma membrane. These data, therefore, suggest that the proximity of the flexible linker of ISG65 to the thioester site of C3b, which occurs due to the interaction of ISG65 with C3/C3b, increases the likelihood of the thioester domain coming into contact with the ISG65 C-terminal linker, leading to the formation of a preferential conjugate between ISG65 and C3b. Indeed, as ISG65 can interact with C3 before conversion to C3b generates the reactive thioester, this conjugate may be preferred over conjugation of C3b to VSG, acting as a decoy to reduce the conjugation of C3b to other regions of the trypanosome surface. Whether this occurs on a trypanosome surface requires further experimentation.

ISG65 blocks the binding of complement receptors 2 and 3 to C3b and C3d

As the central component of the complement system, C3 is the target of many host-proteins (Ricklin *et al.*, 2016). These factors can be broadly grouped into the complement receptors, which are found on immune cells and bind to C3b, iC3b, C3db, and C3d fragments, and factors that regulate the activity of C3b. Complement regulators typically act by blocking recognition of C3b by host-factors to prevent downstream activation (Noris and Remuzzi, 2013). To test whether ISG65 might influence the capacity of complement regulators and receptors to bind to C3b/d, we next compared the structure of ISG65-bound C3b with previously determined structures of C3b and C3d bound to different complement regulators and receptors (Figure 4).

The conformation and location of ISG65 bound to C3d demonstrates that ISG65 binding would preclude binding of Factor H domains 19–20 (Morgan *et al.*, 2011; Figure 4). In addition, ISG65 is predicted to have different effects on binding of complement receptors to C3b. The binding site on C3b for ISG65 does not overlap with those for C3b-binding complement receptors CR1g (Wiesmann *et al.*, 2006) and CR1 (Forneris *et al.*, 2016). However, the region on C3d occupied by ISG65 overlaps with sites on the TED domain/C3d which bind complement receptors 2 (CR2) (van den Elsen and Isenman, 2011) and 3 (CR3) (Bajic *et al.*, 2013; Figure 4). CR2 is a receptor found on B cells, which in

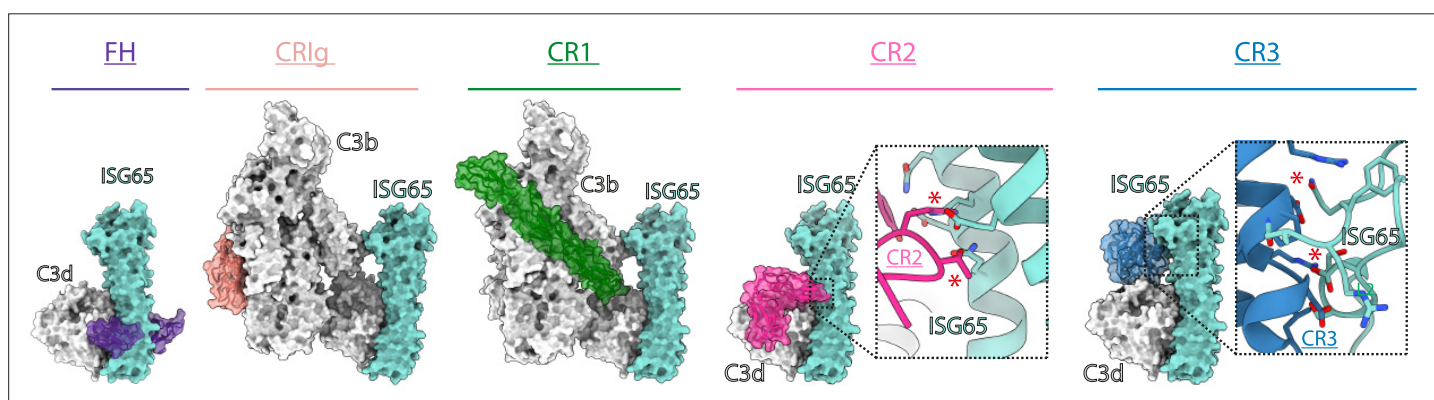


Figure 4. ISG65 overlaps the binding sites for complement receptors 2 and 3. Composite models obtained by docking the C3b-ISG65 structure onto those of C3b/d bound to factor H CCP19-20 (3OXU) (Morgan *et al.*, 2011), CR1g (2ICF) (Wiesmann *et al.*, 2006), CR1 CCP15-17 (5FO9) (Forneris *et al.*, 2016), CR2 SCR1-2 (3OED) (van den Elsen and Isenman, 2011) and CR3 I-domain (4M76) (Bajic *et al.*, 2013). C3b/d is shown in a solid light grey surface, ISG65 is shown in a solid turquoise surface, and complement regulators are shown in transparent surface with ribbon in various colours.

The online version of this article includes the following figure supplement(s) for figure 4:

Figure supplement 1. Comparison of ISG65 sequences from *T. brucei brucei* (green labels), *T. brucei rhodesiense* (blue labels), and *T. brucei gambiense* (red labels).

complex with CD19 and CD81, forms a signal transducing B-cell co-receptor (**Bradbury et al., 1992**). Binding of C3d to CR2 greatly reduces the threshold for B cell activation, thereby triggering B cell activation and antibody production (**Croix et al., 1996**). By preventing VSG-conjugated C3b from binding to B cells through an interaction mediated by CR2, ISG65 may reduce the likelihood that C3b-conjugated trypanosomes will induce B-cell activation and antibody production. Similarly, the binding site for CR3 on C3d also overlaps with that for ISG65, suggesting that ISG65 will block CR3 binding. CR3 is widely expressed on various immune cells and is known to promote macrophage recruitment and phagocytosis by binding to iC3b/C3d, indicating that ISG65 may help reduce trypanosome clearance by blocking this interaction (**Erdei et al., 2019**).

Discussion

The long-term survival of a pathogen in a mammalian host can only occur if it has evolved strategies to avoid clearance by all arms of the host immune system, including the complement system. In a previous study, we highlighted the importance of the complement system in the clearance of trypanosomes during the first wave of infection in a mammalian infection model (**Macleod et al., 2022**). Mice infected with trypanosomes showed two waves of infection. The first peaked around five days after infection and was partially controlled. Around eight days after infection, a second wave was initiated, most likely due to trypanosomes which had undergone antigenic variation through switching their VSG coat. When a similar infection experiment was conducted using the same trypanosome cell line to infect mice lacking complement C3, then the first wave of infection was no longer controlled. This suggested that control of the first wave of infection was mediated by both antibodies and by complement, implicating the classical complement pathway. When wild-type mice were infected with trypanosomes lacking the complement C3/C3b receptor, ISG65, the control of the first wave of infection was delayed, suggesting that ISG65 reduces the susceptibility of trypanosomes to destruction by complement (**Macleod et al., 2022**). However, this study did not investigate the molecular mechanism by which ISG65 reduces the activity of complement.

Our previous structural studies revealed that ISG65 binds to C3d, which is equivalent to the isolated TED domain of C3b (**Macleod et al., 2022**). However, they also suggested that this does not describe the full interaction interface between ISG65 and C3b, with ISG65 showing a ~10 fold higher affinity for C3b than it shows for C3d (**Macleod et al., 2022**). To understand the molecular mechanism for ISG65 function, we therefore needed to reveal the full C3b binding mode of ISG65. We now show, through cryogenic electron microscopy, that in addition to interacting with the TED domain, ISG65 also interacts with the CUB domain of C3b, simultaneously bridging these two sites with a second structure, of C3b bound to ISG65 from *T. b. gambiense*, giving the same conclusion (**Sülzen et al., 2023**). Indeed, there are no consistent differences between the ISG65 receptors from *T. brucei* and its human-infective subspecies, *T. b. gambiense* and *T. b. rhodesiense* (**Figure 4—figure supplement 1**), making it highly likely that ISG65 functions in the same way in human and bovine-infective trypanosomes. This complete model of the ISG65-C3b complex now allows us to answer a series of questions about how ISG65 might modulate C3b function, showing whether ISG65 prevents the formation of C3b, whether it blocks formation of the C3 convertase and whether it blocks the binding of complement regulators and complement receptors to C3b.

The first conclusion is that ISG65 does not prevent the conformational changes which occur as C3 is converted to C3b, with no difference in conformation of free C3b and ISG65-bound C3b. Neither does ISG65 prevent the formation of the C3 convertase, C3bBb. This convertase forms when C3b recruits factors B and D, leading to cleavage of factor B to generate fragments Ba and Bb, with Bb remaining bound to C3b (**Gros et al., 2008**). The C3bBb convertase can then induce the formation of more C3b from C3, thereby increasing the quantity of surface-bound C3b and amplifying the complement cascade. ISG65 does not block the binding sites occupied by factors B or D, or the site proposed to be occupied by subsequent C3 molecules (**Rooijackers et al., 2009**). Indeed, in a solution assay to measure C3 convertase function, we see that the presence of ISG65 has no effect on C3bBb activity. Indeed, two other reports, using different assays, also find no inhibition of C3 convertase formation by ISG65 (**Sülzen et al., 2023; Lorentzen et al., 2023**).

Intriguingly, while ISG65 does not affect C3 convertase function in this solution assay, we find that a newly formed conjugate is established between the flexible C-terminal tail of ISG65 and newly formed C3b. Indeed, the location of the C-terminal tail places it close to the thioester-forming residue in the

context of the ISG65-C3b complex. This conjugate is not formed when BSA is included in the assay at a similar concentration, or when ISG65 lacking the C-terminal tail is used. Could the formation of this conjugate help to protect the trypanosome from the downstream effects of C3b deposition on the cell surface? The amplification of C3b deposition, and the subsequent formation of the C5 convertase, requires C3b molecules and their binding partners to come into close proximity. It is possible that conjugating C3b to ISG65, which will swing above the trypanosome surface on a flexible linker, might make the C3b molecules less likely to come together productively than if they were linked to sites in the VSG surface.

Finally, our complete ISG65-C3b structure shows which binding sites for other complement receptors and regulators are occluded by the presence of ISG65. Indeed, we find that the binding sites on C3b and C3d for complement receptors 2 and 3 overlap with that of ISG65. These receptors are found on B cells and leukocytes, respectively. By blocking CR2 binding, ISG65 is likely to reduce B cell activation and antibody production, while blocking CR3 binding is likely to reduce trypanosome clearance by phagocytosis and complement-mediated cytotoxicity.

Therefore, our studies suggest that ISG65 might dampen the outcomes of the complement system through a diverse combination of mechanisms. By enhancing its affinity for C3b through a two-site binding mechanism, ISG65 will preferentially partition onto cell surface conjugated C3b than soluble C3. When ISG65 binds to C3 or C3b which is approaching the cell surface, a conjugate will preferentially be formed between the C-terminal tail of ISG65 and C3b, ensuring that C3b is flexibly attached rather than more rigidly associated with VSG, perhaps altering the likelihood of it forming productive complexes, such as C5 convertases. Finally, ISG65 may bind to VSG-conjugated C3b, blocking recruitment and stimulation of immune cells by the trypanosome surface, by preventing binding of CR2 and CR3. Other recent publications suggest that ISG65 might also inhibit formation of the C5 convertase (Sülzen *et al.*, 2023) or accelerate the decay of C3b to iC3b (Lorentzen *et al.*, 2023). Each of these effects could contribute to dampening of the complement response, while rapid clearance of surface attached C3b through hydrodynamic forces resulting from trypanosome swimming, coupled with rapid endocytosis, cleans the trypanosome surface.

While a number of functions have been ascribed to ISG65, it is noteworthy that none of the studies to date assess its function in the unusual context of a VSG-coated trypanosome surface, which may limit formation of the membrane attack complex and operation of the alternative pathway of complement (Cook *et al.*, 2023). It will, therefore, be important for future studies to determine whether each of the functions proposed for ISG65, observed in *in vitro* assays, are also operational on trypanosomes before we can fully understand how ISG65 helps trypanosomes to survive.

Methods

Key resources table

Reagent type (species) or resource	Designation	Source or reference	Identifiers	Additional information
Gene (<i>Trypanosoma brucei brucei</i>)	ISG65G gene	NCBI BioProject Accession: PRJEB46985	UniProt: A0A8J9S0Z8	
Gene (<i>Homo sapiens</i>)	CFB gene	NCBI GenBank accession: AF019413.1	UniProt: P00751	
Gene (<i>H. sapiens</i>)	CFD gene	NCBI GenBank accession: CH471139.2	UniProt: P00746	
Gene (<i>H. sapiens</i>)	C3 gene	NCBI GenBank accession: AY513239.1	UniProt: P01024	
Sequence-based reagent	Primers	This paper		See list of primers in the Appendix. Primers were synthesised by Sigma.
Recombinant DNA reagent	pHL-SEC vector backbone	https://doi.org/10.1107/S0907444906029799 ; Aricescu <i>et al.</i> , 2006		
Cell line (<i>H. sapiens</i>)	HEK293F	Gibco	R79007	
Biological sample (<i>H. sapiens</i>)	Human serum	NHSBT non-clinical issue		
Software	SIMPLE v3	https://github.com/hael/SIMPLE/releases ; Elmlund <i>et al.</i> , 2020		

Continued on next page

Continued

Reagent type (species) or resource	Designation	Source or reference	Identifiers	Additional information
Software	CryoSPARC v3	https://cryosparc.com/ ; <i>Structura Biotechnology Inc, 2020</i>		
Software	TOPAZ v0.2.4	https://github.com/tbepler/topaz ; <i>Bepler and Noble, 2020</i>		
Software	RELION v3.1	https://relion.readthedocs.io/en/release-3.1/index.html ; <i>RELION developer team, 2020</i>		
Software	DeepEMhancer	https://github.com/rsanchezgarc/deepEMhancer ; <i>Sanchez Garcia, 2022</i>		
Software	AlphaFold2	https://github.com/google-deepmind/alphafold ; <i>AlphaFold Team, 2021</i>		
Software	ISOLDE v1.0	https://github.com/tristanic/isolde ; <i>Croll, 2019</i>		
Software	COOT v0.9.8.3	https://github.com/pemsley/coot ; <i>Emsley, 2022</i>		
Software	PHENIX v1.20.1	https://phenix-online.org/ ; <i>Phenix Development Group, 2022</i>		
Software	ChimeraX v1.6	https://www.cgl.ucsf.edu/chimerax/ ; <i>UCSF Resource for Biocomputing, Visualization, and Informatics, 2023</i>		
Software	BIAevaluation v1.0	Biacore, Cytiva, Marlborough, MA, USA		
Software	Fiji	https://imagej.net/software/fiji/		

Mammalian expression and purification of ISG65 and complement proteins

To express ISG65 1125 G (*Macleod et al., 2022*) (residues 24–385), we used a pDest12 plasmid consisting of an N-terminal secretion signal, codon-optimized ISG65, a C-terminal flexible linker (GSGSGSASG), AviTag, and a His₁₀-tag. Human Complement Factor B (residues 26–764) and Complement Factor D (residues 20–253) were cloned into a pHlsec plasmid containing an N-terminal secretion signal and a short C-terminal linker (GSG) followed by a C-tag. ISG65, Factor B, and Factor D DNA were transfected into HEK293F cells (3 µg DNA per mL of cells) grown in F17 Freestyle media to a density of 2.2×10⁶ cells/mL, using polyethylenimine (9 µg per mL of cells). Media was supplemented with 1 µM kifunensine and 3.8 mM valproic acid. Cell culture supernatant was harvested 6 days after transfection. Initial purification of ISG65 was performed using Ni Sepharose excel resin (Cytiva), whilst CaptureSelect C-tagXL Affinity Matrix (Thermo Fisher) was used to purify Factor B and D. ISG65 and Factor D were further purified on a Superdex 75 300/10 (Cytiva), whilst Factor B was further purified with a Superdex 200 300/10 (Cytiva). ISG65 loops deletions (loop1: ΔP88-K92insSS, loop2: ΔQ155-R195, loop3: ΔK230-P250, tail: ΔK317-G394), and ISG65^{N188A,H189A,Y190A} were generated using Gibson Assembly (NEB) and expressed and purified as described for ISG65 24–385 above. ISG65 and ISG65ΔL2 were biotinylated on their C-terminal AviTag using the Enzymatic Biotinylated Kit (Sigma).

Purification of human complement C3 and C3d, and generation of C3b

To purify Complement C3, anonymous donor post-clot human serum was obtained from the NHS Blood and Transplant non-clinical issue supply. Serum was buffer exchanged into 20 mM Tris pH 8, 50 mM NaCl, and 0.5 mM EDTA using tangential flow filtration with a stack of three 100 kDa Omega Cassettes (PALL Corporation). Serum was clarified by ultra-centrifugation at 41,000 rpm in a Ti-45 rotor (Beckman Coulter). Purification of C3 was performed by anion exchange chromatography using a HiPrep Q HP 16/60 column (Cytiva) with a 20-column volume gradient of 50–350 mM NaCl. Fractions containing C3 were pooled then buffer exchanged into 20 mM MES pH 6, 50 mM NaCl, and 0.5 mM EDTA using tangential flow filtration as above. C3 was then purified by cation exchange using a monoS 4.6/100 PE (Cytiva) with a 30-column volume gradient to 500 mM NaCl. Fractions containing C3 were then further purified on a Superdex 200 300/10.

C3b was generated from C3 by limited proteolysis with trypsin (Roche) at 1 % w/w trypsin to C3 at 37 °C for 2 min. Trypsin was then inhibited with soybean trypsin inhibitor (Merck) at a ratio of 1 % w/w inhibitor to C3. For biotinylation of C3b, 100 mM HEPES pH 7.0 was added after addition of soybean trypsin inhibitor, followed by a 10-fold molar excess of maleimide-PEG2-biotin (ThermoFisher). The reaction was incubated on ice for 6 hr. C3b or biotin-C3b was then purified on a Superdex 100 300/10.

We previously expressed C3d with a C1010A mutation to prevent formation of thioester bonds (Macleod *et al.*, 2022). To generate C3d with a single biotin in proximity to the thioester-forming Gln¹⁰¹³ residue, we generated a Q1013A mutation in C3d which prevented thioester bond formation but left Cys¹⁰¹⁰ exposed. C3d^{Q1013A} was expressed in *E. coli* as previously described for the C1010A mutant (Macleod *et al.*, 2022) and was then reacted with maleimide-PEG2-biotin, as described above for C3b.

Preparation of ISG65-C3b complexes for cryo-EM

To form C3b-ISG65 complexes, C3b was mixed with ISG65 at a 1:1.1 ratio in 20 mM HEPES pH 7.4, 150 mM NaCl, and 0.5 mM EDTA. Complexes were then purified on a Superdex 200 300/10 GL column. Quantifoil grids consisting of a 1.2/1.3 µm holey carbon film on 300 gold mesh were glow discharged at 15 mA for 1 min with an EM ACE200 glow discharger (Leica). Just before vitrification, 0.01% fluorinated octyl maltoside (Anatrace) was added to 2.2 mg/mL C3b-ISG65, which was then immediately added to the grid and plunge frozen in an ethane slush using a Vitrobot Mark IV (Thermo Fisher). Grids were imaged with a Titan Krios G2 (Thermo Fisher) operating at 300 kV, and images were recorded with a K3 detector (Gatan) in counting mode with a GIF Quantum LS Imaging Filter (Gatan).

Image processing and modelling of ISG65-C3b complexes

Movies were motion-corrected, contrast transfer function (CTF) corrected, and particles were picked using SIMPLE v3 (Caesar *et al.*, 2020) on the fly. To obtain an initial set of C3b/C3b-ISG65 particles, one round of 2D classification was performed in SIMPLE, followed by another two rounds of 2D classification in CryoSPARC v3 (Punjani *et al.*, 2017). A second set of particles was obtained by particle picking with TOPAZ v0.2.4 Bepler *et al.*, 2019 followed by one round of 2D classification to remove bad particles. TOPAZ and SIMPLE particles were combined, duplicates removed, and a final round of 2D classification was performed. Three rounds of *ab initio* and heterogeneous 3D refinement were performed in CryoSPARC using 5 classes which resulted in a set of C3b-ISG65 particles, and a set of C3b only particles. Both particle sets were merged and yielded a 3.5 Å map from homogenous refinement in CryoSPARC. Bayesian polishing was then performed in Relion v3.1 (Zivanov *et al.*, 2018; Zivanov *et al.*, 2019), followed by per particle CTF refinement and beam tilt estimation in CryoSPARC, yielding a 3.3 Å map. Particles were separated into C3b-ISG65 and C3b only sets, yielding 3.3 and 3.4 Å resolution maps, respectively. The resolution of CUB, TED, and ISG65 were significantly lower than the rest of the map presumably because of flexibility in CUB and TED, and because of the location of ISG65 on the periphery of the map. To mitigate this, particle coordinates were shifted such that CUB-TED-ISG65 density was in the middle of the box, then all density other than CUB-TED-ISG65 was subtracted using a 10-pixel soft edge mask. Local refinement was then performed using a pose/shift Gaussian prior with a standard deviation of 3° over rotations and 2 Å over shifts, and search limitations of 12° and 9 Å, resulting in a 3.4 Å map. Local refinement was also performed for all density except CUB-C3d-ISG65 using a 15-pixel soft edge mask, yielding a 3.2 Å map. Post-processing was then performed using DeepEMhancer, and local resolution was estimated with CryoSPARC, and locally refined maps were combined in ChimeraX (Pettersen *et al.*, 2021) to create a composite map.

To generate a model of ISG65-C3b, a previous crystal structure of C3b (PDB ID: 5FO7) (Forneris *et al.*, 2016) and a structure prediction of ISG65 performed with AlphaFold2 (Jumper *et al.*, 2021) were rigid-body fitted into cryo-EM density using the fit-in map tool in ChimeraX (Pettersen *et al.*, 2021). Refinement of C3b-ISG65 was then performed using ISOLDE v1.0 (Croll, 2018), COOT v0.9.8.3 (Emsley *et al.*, 2010), and Phenix v1.20.1 (Liebschner *et al.*, 2019).

Surface plasmon resonance

SPR experiments were performed on a BIACore T200 (Cytiva). Biotin-C3b or biotin-C3d were immobilised on the SPR chip via streptavidin using a CAPture kit (Cytiva). Two-fold serial dilutions of ISG65,

ISG65 Δ L2, and ISG65^{N188A,H189A,Y190A} were injected over the chip. Measurements were performed at 30 μ L/min at 25 °C in 20 mM HEPES pH 7.4, 150 mM NaCl, 0.05% TWEEN-20, with an association and dissociation time of 120 s. Binding responses were obtained using BIAevaluation software v1.0, followed by fitting to a 1:1 Langmuir model. Three experimental replicates of SPR experiments were performed, including two biological replicates of ISG65, biotin-C3d, and biotin-C3b.

C3 convertase activity assays

To measure the effect of ISG65 on C3 convertase activity, 600 nM C3, 600 nM Factor B, 12 nM C3b, 12 nM Factor D, and 2 μ M ISG65 or 2 μ M bovine serum albumin (Sigma) were combined in phosphate-buffered saline pH 7.4, 2 mM MgCl₂. The reaction was carried out at 22 °C and samples were removed at various intervals and combined with SDS-PAGE sample buffer before running on SDS-PAGE to assess band shifts in C3 and Factor B. Gel densitometry was performed in Fiji (*Schindelin et al., 2012*).

Acknowledgements

This work was funded through a Wellcome Investigator award (217138/Z/19/Z). We thank Olivia MacLeod for discussions about the complement system and its regulation and Rishi Matadeen, Joseph Caesar, and Teige Matthews-Palmer at the COSMIC cryo-EM facility (University of Oxford) for support with data collection and data processing.

Additional information

Funding

Funder	Grant reference number	Author
Wellcome Trust	217138/Z/19/Z	Alexander D Cook Mark Carrington Matthew K Higgins

The funders had no role in study design, data collection and interpretation, or the decision to submit the work for publication. For the purpose of Open Access, the authors have applied a CC BY public copyright license to any Author Accepted Manuscript version arising from this submission.

Author contributions

Alexander D Cook, Conceptualization, Data curation, Formal analysis, Investigation, Methodology, Writing - original draft, Writing - review and editing; Mark Carrington, Conceptualization, Formal analysis, Funding acquisition, Writing - original draft, Writing - review and editing; Matthew K Higgins, Conceptualization, Formal analysis, Supervision, Funding acquisition, Writing - original draft, Writing - review and editing

Author ORCIDs

Mark Carrington  <http://orcid.org/0000-0002-6435-7266>
Matthew K Higgins  <http://orcid.org/0000-0002-2870-1955>

Peer review material

Reviewer #1 (Public Review): <https://doi.org/10.7554/eLife.88960.3.sa1>
Reviewer #3 (Public Review): <https://doi.org/10.7554/eLife.88960.3.sa2>
Author response <https://doi.org/10.7554/eLife.88960.3.sa3>

Additional files

Supplementary files

- Supplementary file 1. Supplementary Table 1: Cryo-EM data collection and model building statistics.
- Supplementary file 2. Supplementary Table 2: Kinetic parameters of ISG65 variants binding to biotinylated C3b and C3d, as measured by surface plasmon resonance. Average values and standard

deviation from three experimental repeats are reported.

- Supplementary file 3. Supplementary Table 3: Mass spectrometry analysis of ISG65-C3b conjugates observed in **Figure 3**. The high molecular weight band observed in convertase assay in the presence of ISG65 was excised and analysed by mass spectrometry. The three most abundant proteins identified are presented.
- Supplementary file 4. Primers.
- MDAR checklist

Data availability

Cryo-EM maps are available from the Electron Microscopy Data Bank under accession codes EMDB-17209 (C3b-ISG65 composite map), EMDB-17219 (locally aligned CUB-TED-ISG65), EMDB-17220 (locally aligned C3c region), EMDB-17221 (C3b only) and EMDB-17273 (consensus map), while coordinates for C3b-ISG65 are available from the Protein Data Bank under accession code 8OVB.

The following datasets were generated:

Author(s)	Year	Dataset title	Dataset URL	Database and Identifier
Cook AD, Higgins MK	2024	Human Complement C3b in complex with <i>Trypanosoma brucei</i> ISG65	https://www.rcsb.org/structure/8OVB	RCSB Protein Data Bank, 8OVB
Cook AD, Higgins MK	2024	Human Complement C3b in complex with <i>Trypanosoma brucei</i> ISG65	https://www.ebi.ac.uk/emdb/EMD-17209	EMDataBank, EMD-17209
Cook AD, Higgins MK	2024	Human Complement C3b in complex with <i>Trypanosoma brucei</i> ISG65	https://www.ebi.ac.uk/emdb/EMD-17219	EMDataBank, EMD-17219
Cook AD, Higgins MK	2024	Human Complement C3b in complex with <i>Trypanosoma brucei</i> ISG65	https://www.ebi.ac.uk/emdb/EMD-17220	EMDataBank, EMD-17220
Cook AD, Higgins MK	2024	Human Complement C3b	https://www.ebi.ac.uk/emdb/EMD-17221	EMDataBank, EMD-17221
Cook AD, Higgins MK	2024	Structure of complement C3 bound to <i>Trypanosoma brucei</i> ISG65	https://www.ebi.ac.uk/emdb/EMD-17273	EMDataBank, EMD-17273

References

- AlphaFold Team.** 2021. AlphaFold2. v2.0.0. GitHub. <https://github.com/google-deepmind/alphafold>
- Aricescu AR, Lu W, Jones EY.** 2006. A time- and cost-efficient system for high-level protein production in mammalian cells. *Acta Crystallographica Section D Biological Crystallography* **62**:1243–1250. DOI: <https://doi.org/10.1107/S0907444906029799>
- Bajic G, Yatime L, Sim RB, Vorup-Jensen T, Andersen GR.** 2013. Structural insight on the recognition of surface-bound opsonins by the integrin I domain of complement receptor 3. *PNAS* **110**:16426–16431. DOI: <https://doi.org/10.1073/pnas.1311261110>, PMID: 24065820
- Bepler T, Morin A, Rapp M, Brasch J, Shapiro L, Noble AJ, Berger B.** 2019. Positive-unlabeled convolutional neural networks for particle picking in cryo-electron micrographs. *Nature Methods* **16**:1153–1160. DOI: <https://doi.org/10.1038/s41592-019-0575-8>, PMID: 31591578
- Bepler T, Noble AJ.** 2020. TOPAZ. v0.2.4. GitHub. <https://github.com/tbepler/topaz>
- Bradbury LE, Kansas GS, Levy S, Evans RL, Tedder TF.** 1992. The CD19/CD21 signal transducing complex of human B lymphocytes includes the target of antiproliferative antibody-1 and Leu-13 molecules. *Journal of Immunology* **149**:2841–2850 PMID: 1383329.
- Caesar J, Reboul CF, Machello C, Kiesewetter S, Tang ML, Deme JC, Johnson S, Elmlund D, Lea SM, Elmlund H.** 2020. SIMPLE 3.0. Stream single-particle cryo-EM analysis in real time. *Journal of Structural Biology* **4**:100040. DOI: <https://doi.org/10.1016/j.jysbx.2020.100040>, PMID: 33294840
- Capron M, Kazatchkine MD, Fischer E, Joseph M, Butterworth AE, Kusnierz JP, Prin L, Papin JP, Capron A.** 1987. Functional role of the alpha-chain of complement receptor type 3 in human eosinophil-dependent antibody-mediated cytotoxicity against schistosomes. *Journal of Immunology* **139**:2059–2065 PMID: 2957447.
- Clark EA, Crennell S, Upadhyay A, Zozulya AV, Mackay JD, Svergun DI, Bagby S, van den Elsen JMH.** 2011. A structural basis for Staphylococcal complement subversion: X-ray structure of the complement-binding domain of *Staphylococcus aureus* protein Sbi in complex with ligand C3d. *Molecular Immunology* **48**:452–462. DOI: <https://doi.org/10.1016/j.molimm.2010.09.017>, PMID: 21055811

- Cook AD**, Carrington M, Higgins MK. 2023. Molecular Mechanism of Complement Inhibition by the Trypanosome Receptor ISG65. *bioRxiv*. DOI: <https://doi.org/10.1101/2023.04.27.538609>
- Couves EC**, Gardner S, Voisin TB, Bickel JK, Stansfeld PJ, Tate EW, Bubeck D. 2023. Structural basis for membrane attack complex inhibition by CD59. *Nature Communications* **14**:890. DOI: <https://doi.org/10.1038/s41467-023-36441-z>, PMID: 36797260
- Croix DA**, Ahearn JM, Rosengard AM, Han S, Kelsoe G, Ma M, Carroll MC. 1996. Antibody response to a T-dependent antigen requires B cell expression of complement receptors. *The Journal of Experimental Medicine* **183**:1857–1864. DOI: <https://doi.org/10.1084/jem.183.4.1857>, PMID: 8666942
- Croll TI**. 2018. ISOLDE: a physically realistic environment for model building into low-resolution electron-density maps. *Acta Crystallographica. Section D, Structural Biology* **74**:519–530. DOI: <https://doi.org/10.1107/S2059798318002425>, PMID: 29872003
- Croll T**. 2019. ISOLDE. v1.0. GitHub. <https://github.com/tristanic/isolde>
- Emlund H**, Reboul C, cong. 2020. SIMPLE. v3. GitHub. <https://github.com/hael/SIMPLE/>
- Emsley P**, Lohkamp B, Scott WG, Cowtan K. 2010. Features and development of Coot. *Acta Crystallographica. Section D, Biological Crystallography* **66**:486–501. DOI: <https://doi.org/10.1107/S0907444910007493>, PMID: 20383002
- Emsley P**. 2022. COOT. v0.9.8.3. GitHub. <https://github.com/pemsley/coot>
- Erdei A**, Lukácsi S, Mácsik-Valent B, Nagy-Baló Z, Kurucz I, Bajtay Z. 2019. Non-identical twins: Different faces of CR3 and CR4 in myeloid and lymphoid cells of mice and men. *Seminars in Cell & Developmental Biology* **85**:110–121. DOI: <https://doi.org/10.1016/j.semcdb.2017.11.025>, PMID: 29174917
- Fischer MB**, Goerg S, Shen L, Prodeus AP, Goodnow CC, Kelsoe G, Carroll MC. 1998. Dependence of germinal center B cells on expression of CD21/CD35 for survival. *Science* **280**:582–585. DOI: <https://doi.org/10.1126/science.280.5363.582>, PMID: 9554848
- Forneris F**, Ricklin D, Wu J, Tzekou A, Wallace RS, Lambris JD, Gros P. 2010. Structures of C3b in complex with factors B and D give insight into complement convertase formation. *Science* **330**:1816–1820. DOI: <https://doi.org/10.1126/science.1195821>, PMID: 21205667
- Forneris F**, Wu J, Xue X, Ricklin D, Lin Z, Sfyroera G, Tzekou A, Volokhina E, Granneman JC, Hauhart R, Bertram P, Liszewski MK, Atkinson JP, Lambris JD, Gros P. 2016. Regulators of complement activity mediate inhibitory mechanisms through a common C3b-binding mode. *The EMBO Journal* **35**:1133–1149. DOI: <https://doi.org/10.15252/embj.201593673>, PMID: 27013439
- Gros P**, Milder FJ, Janssen BJC. 2008. Complement driven by conformational changes. *Nature Reviews. Immunology* **8**:48–58. DOI: <https://doi.org/10.1038/nri2231>, PMID: 18064050
- Hammel M**, Sfyroera G, Ricklin D, Magotti P, Lambris JD, Geisbrecht BV. 2007. A structural basis for complement inhibition by *Staphylococcus aureus*. *Nature Immunology* **8**:430–437. DOI: <https://doi.org/10.1038/ni1450>, PMID: 17351618
- Ismenman DE**, Leung E, Mackay JD, Bagby S, van den Elsen JMH. 2010. Mutational analyses reveal that the staphylococcal immune evasion molecule Sbi and complement receptor 2 (CR2) share overlapping contact residues on C3d: implications for the controversy regarding the CR2/C3d cocrystal structure. *Journal of Immunology* **184**:1946–1955. DOI: <https://doi.org/10.4049/jimmunol.0902919>, PMID: 20083651
- Janssen BJC**, Huizinga EG, Raaijmakers HCA, Roos A, Daha MR, Nilsson-Ekdahl K, Nilsson B, Gros P. 2005. Structures of complement component C3 provide insights into the function and evolution of immunity. *Nature* **437**:505–511. DOI: <https://doi.org/10.1038/nature04005>, PMID: 16177781
- Janssen BJC**, Christodoulidou A, McCarthy A, Lambris JD, Gros P. 2006. Structure of C3b reveals conformational changes that underlie complement activity. *Nature* **444**:213–216. DOI: <https://doi.org/10.1038/nature05172>, PMID: 17051160
- Jumper J**, Evans R, Pritzel A, Green T, Figurnov M, Ronneberger O, Tunyasuvunakool K, Bates R, Židek A, Potapenko A, Bridgland A, Meyer C, Kohl SAA, Ballard AJ, Cowie A, Romera-Paredes B, Nikolov S, Jain R, Adler J, Back T, et al. 2021. Highly accurate protein structure prediction with AlphaFold. *Nature* **596**:583–589. DOI: <https://doi.org/10.1038/s41586-021-03819-2>, PMID: 34265844
- Lambris JD**, Ricklin D, Geisbrecht BV. 2008. Complement evasion by human pathogens. *Nature Reviews. Microbiology* **6**:132–142. DOI: <https://doi.org/10.1038/nrmicro1824>, PMID: 18197169
- Liebschner D**, Afonine PV, Baker ML, Bunkóczi G, Chen VB, Croll TI, Hintze B, Hung LW, Jain S, McCoy AJ, Moriarty NW, Oeffner RD, Poon BK, Prisant MG, Read RJ, Richardson JS, Richardson DC, Sammito MD, Sobolev OV, Stockwell DH, et al. 2019. Macromolecular structure determination using X-rays, neutrons and electrons: recent developments in Phenix. *Acta Crystallographica. Section D, Structural Biology* **75**:861–877. DOI: <https://doi.org/10.1107/S2059798319011471>, PMID: 31588918
- Lorentzen J**, Olesen HG, Hansen AG, Thiel S, Birkelund S, Andersen CBF, Andersen GR. 2023. *Trypanosoma brucei* Invariant Surface gp65 Inhibits the Alternative Pathway of Complement by Accelerating C3b Degradation. *Journal of Immunology* **211**:862–873. DOI: <https://doi.org/10.4049/jimmunol.2300128>, PMID: 37466368
- Macleod OJS**, Bart JM, MacGregor P, Peacock L, Savill NJ, Hester S, Ravel S, Sunter JD, Trevor C, Rust S, Vaughan TJ, Minter R, Mohammed S, Gibson W, Taylor MC, Higgins MK, Carrington M. 2020. A receptor for the complement regulator factor H increases transmission of trypanosomes to tsetse flies. *Nature Communications* **11**:1326. DOI: <https://doi.org/10.1038/s41467-020-15125-y>, PMID: 32165615
- Macleod OJS**, Cook AD, Webb H, Crow M, Burns R, Redpath M, Seisenberger S, Trevor CE, Peacock L, Schwede A, Kimblin N, Francisco AF, Pepperl J, Rust S, Voorheis P, Gibson W, Taylor MC, Higgins MK,

- Carrington M. 2022. Invariant surface glycoprotein 65 of *Trypanosoma brucei* is a complement C3 receptor. *Nature Communications* **13**:5085. DOI: <https://doi.org/10.1038/s41467-022-32728-9>, PMID: 36038546
- Morgan HP, Schmidt CQ, Guariento M, Blaum BS, Gillespie D, Herbert AP, Kavanagh D, Mertens HDT, Svergun DI, Johansson CM, Uhrin D, Barlow PN, Hannan JP. 2011. Structural basis for engagement by complement factor H of C3b on a self surface. *Nature Structural & Molecular Biology* **18**:463–470. DOI: <https://doi.org/10.1038/nsmb.2018>, PMID: 21317894
- Nilsson B, Nilsson Ekdahl K. 2012. The tick-over theory revisited: is C3 a contact-activated protein? *Immunobiology* **217**:1106–1110. DOI: <https://doi.org/10.1016/j.imbio.2012.07.008>, PMID: 22964236
- Noris M, Remuzzi G. 2013. Overview of complement activation and regulation. *Seminars in Nephrology* **33**:479–492. DOI: <https://doi.org/10.1016/j.semnephrol.2013.08.001>, PMID: 24161035
- Pettersen EF, Goddard TD, Huang CC, Meng EC, Couch GS, Croll TI, Morris JH, Ferrin TE. 2021. UCSF ChimeraX: Structure visualization for researchers, educators, and developers. *Protein Science* **30**:70–82. DOI: <https://doi.org/10.1002/pro.3943>, PMID: 32881101
- Phenix Development Group. 2022. PHENIX. v1.20.1. Phenix. <https://phenix-online.org>
- Punjani A, Rubinstein JL, Fleet DJ, Brubaker MA. 2017. cryoSPARC: algorithms for rapid unsupervised cryo-EM structure determination. *Nature Methods* **14**:290–296. DOI: <https://doi.org/10.1038/nmeth.4169>, PMID: 28165473
- RELION developer team. 2020. RELION. v3.1. GitHub. <https://github.com/3dem/relion>
- Ricklin D, Ricklin-Lichtsteiner SK, Markiewski MM, Geisbrecht BV, Lambris JD. 2008. Cutting edge: members of the *Staphylococcus aureus* extracellular fibrinogen-binding protein family inhibit the interaction of C3d with complement receptor 2. *Journal of Immunology* **181**:7463–7467. DOI: <https://doi.org/10.4049/jimmunol.181.11.7463>, PMID: 19017934
- Ricklin D, Reis ES, Mastellos DC, Gros P, Lambris JD. 2016. Complement component C3 - The “Swiss Army Knife” of innate immunity and host defense. *Immunological Reviews* **274**:33–58. DOI: <https://doi.org/10.1111/imr.12500>, PMID: 27782325
- Roosjakkars SHM, Wu J, Ruyken M, van Domselaar R, Planken KL, Tzekou A, Ricklin D, Lambris JD, Janssen BJC, van Strijp JAG, Gros P. 2009. Structural and functional implications of the alternative complement pathway C3 convertase stabilized by a staphylococcal inhibitor. *Nature Immunology* **10**:721–727. DOI: <https://doi.org/10.1038/ni.1756>, PMID: 19503103
- Rosenthal LA, Sutterwala FS, Kehrl ME, Mosser DM. 1996. Leishmania major-human macrophage interactions: cooperation between Mac-1 (CD11b/CD18) and complement receptor type 1 (CD35) in promastigote adhesion. *Infection and Immunity* **64**:2206–2215. DOI: <https://doi.org/10.1128/iai.64.6.2206-2215.1996>, PMID: 8675328
- Sanchez Garcia R. 2022. DeepEMhancer. v0.14. GitHub. <https://github.com/rsanchezgarc/deepEMhancer>
- Schindelin J, Arganda-Carreras I, Frise E, Kaynig V, Longair M, Pietzsch T, Preibisch S, Rueden C, Saalfeld S, Schmid B, Tinevez J-Y, White DJ, Hartenstein V, Eliceiri K, Tomancak P, Cardona A. 2012. Fiji: an open-source platform for biological-image analysis. *Nature Methods* **9**:676–682. DOI: <https://doi.org/10.1038/nmeth.2019>, PMID: 22743772
- Schwede A, Carrington M. 2010. Bloodstream form *Trypanosoma* plasma membrane proteins: antigenic variation and invariant antigens. *Parasitology* **137**:2029–2039. DOI: <https://doi.org/10.1017/S0031182009992034>, PMID: 20109254
- Schwede A, Macleod OJS, MacGregor P, Carrington M. 2015. How Does the VSG Coat of Bloodstream Form African Trypanosomes Interact with External Proteins? *PLOS Pathogens* **11**:e1005259. DOI: <https://doi.org/10.1371/journal.ppat.1005259>, PMID: 26719972
- Structura Biotechnology Inc. 2020. CryoSPARC. v3. Structura Biotechnology Inc. <https://cryosparc.com/>
- Sudarshi D, Lawrence S, Pickrell WO, Eligar V, Walters R, Quaderi S, Walker A, Capewell P, Clucas C, Vincent A, Checchi F, MacLeod A, Brown M. 2014. Human African trypanosomiasis presenting at least 29 years after infection--what can this teach us about the pathogenesis and control of this neglected tropical disease? *PLOS Neglected Tropical Diseases* **8**:e3349. DOI: <https://doi.org/10.1371/journal.pntd.0003349>, PMID: 25522322
- Sülzen H, Began J, Dhillon A, Kereiche S, Pompach P, Votrubova J, Zahedifard F, Šubrtova A, Šafner M, Hubalek M, Thompson M, Zoltner M, Zoll S. 2023. Cryo-EM structures of *Trypanosoma brucei* gambiense ISG65 with human complement C3 and C3b and their roles in alternative pathway restriction. *Nature Communications* **14**:2403. DOI: <https://doi.org/10.1038/s41467-023-37988-7>, PMID: 37105991
- Tegla CA, Cudrici C, Patel S, Trippe R, Rus V, Niculescu F, Rus H. 2011. Membrane attack by complement: the assembly and biology of terminal complement complexes. *Immunologic Research* **51**:45–60. DOI: <https://doi.org/10.1007/s12026-011-8239-5>, PMID: 21850539
- UCSF Resource for Biocomputing, Visualization, and Informatics. 2023. ChimeraX. v1.6. UCSF. <https://www.cgl.ucsf.edu/chimerax/>
- van den Elsen JMH, Isenman DE. 2011. A crystal structure of the complex between human complement receptor 2 and its ligand C3d. *Science* **332**:608–611. DOI: <https://doi.org/10.1126/science.1201954>, PMID: 21527715
- Wang S, Ma JZ, Xu JB. 2016. AUCpreD: proteome-level protein disorder prediction by AUC-maximized deep convolutional neural fields. *Bioinformatics* **32**:i672–i679. DOI: <https://doi.org/10.1093/bioinformatics/btw446>, PMID: 27587688
- Wiesmann C, Katschke KJ, Yin J, Helmy KY, Steffek M, Fairbrother WJ, McCallum SA, Embuscado L, DeForge L, Hass PE, van Lookeren Campagne M. 2006. Structure of C3b in complex with CR1g gives insights into

- regulation of complement activation. *Nature* **444**:217–220. DOI: <https://doi.org/10.1038/nature05263>, PMID: [17051150](https://pubmed.ncbi.nlm.nih.gov/17051150/)
- Zipfel PF**, Hallström T, Riesbeck K. 2013. Human complement control and complement evasion by pathogenic microbes—tipping the balance. *Molecular Immunology* **56**:152–160. DOI: <https://doi.org/10.1016/j.molimm.2013.05.222>, PMID: [23810413](https://pubmed.ncbi.nlm.nih.gov/23810413/)
- Zivanov J**, Nakane T, Forsberg BO, Kimanius D, Hagen WJ, Lindahl E, Scheres SH. 2018. New tools for automated high-resolution cryo-EM structure determination in RELION-3. *eLife* **7**:e42166. DOI: <https://doi.org/10.7554/eLife.42166>, PMID: [30412051](https://pubmed.ncbi.nlm.nih.gov/30412051/)
- Zivanov J**, Nakane T, Scheres SHW. 2019. A Bayesian approach to beam-induced motion correction in cryo-EM single-particle analysis. *IUCrJ* **6**:5–17. DOI: <https://doi.org/10.1107/S205225251801463X>, PMID: [30713699](https://pubmed.ncbi.nlm.nih.gov/30713699/)